NASA TECHNICAL NOTE

NASA TN D-2749

NASA TN D-2749

DYNAMICS OF A ROTATING CYLINDRICAL SPACE STATION

by Walter Krause Polstorff

George C. Marshall Space Flight Center
Huntsville, Ala.

NATIONAL AERONAUTICS AND SPACE ADMINISTRATION • WASHINGTON, D. C. • APRIL 1965

NASA TN D-2749

DYNAMICS OF A ROTATING CYLINDRICAL SPACE STATION

By Walter Krause Polstorff

George C. Marshall Space Flight Center
Huntsville, Ala.

NATIONAL AERONAUTICS AND SPACE ADMINISTRATION

For sale by the Clearinghouse for Federal Scientific and Technical Information
Springfield, Virginia 22151 – Price $1.00

TABLE OF CONTENTS

LIST OF ILLUSTRATIONS

DEFINITION OF SYMBOLS

Symbol	Definition
X, Y, Z	Space-fixed reference axes
ϕ, θ, ψ	Euler angles
x, y, z	Body-fixed axes
$\overline{H}$	Angular impulse
$\overline{\Omega}$	Angular velocity
$\tilde{I}$	Inertia tensor
I	Moment of inertia
p, q, r	Components of angular velocity in body-fixed coordinate system
D	Determinant
ξ, η, ζ	Principal axes
Φ, Θ, Ψ	Euler angles between principal axes and reference axes
T	Period
m	Movable mass within space station
$\overline{\rho}$	Radius vector of movable mass
$\overline{R}$	Radius vector of center of gravity in body-fixed coordinate system
M	Total mass of space station
$\overline{r}_i$	Position of vector of mass point in space-fixed coordinate system
v	Velocity
h	Angular impulse of rotating machinery
P	Power
L	Torque
E	Energy
α, β, γ	Euler angles between principal axes and body-fixed axes
Ω_ξ, Ω_η, Ω_ζ	Components of angular velocity in principal axis system

DEFINITION OF SYMBOLS (Continued)

Subscripts	Definition
c	Of command
F	Of flywheel

A dot over a symbol denotes the first derivative with respect to time.

Two dots over a symbol denote the second derivative with respect to time.

A bar over a symbol denotes a vector.

A tilde (~) over a symbol denotes a matrix.

DYNAMICS OF A ROTATING CYLINDRICAL SPACE STATION

SUMMARY

Equations describing the reaction of a space vehicle to rotating machinery and to mass motion inside the vehicle are formulated. These equations include a component that has been neglected in most earlier studies, i.e., the angular impulse introduced by the moving mass. The dynamics of a cylindrical space station rotating around its major axis once every 10 seconds are evaluated numerically. The long cylinder provides the large distance between the axis of rotation and the crew compartment needed to generate comfortable artificial gravity. But the rotating cylinder is known to have little dynamic stability around its longitudinal axis. Nevertheless, the stability characteristics of this configuration are found to be acceptable provided there is as little as 0.2% asymmetry between the major and intermediate moments of inertia. Detailed investigations were performed on an analog computer. These show the effect of path and timing on the magnitude of the disturbance caused by a mass relocation. Also analyzed in some detail are ways to minimize roll, either by corrective motion of the astronauts or by a simple control system that uses the gyroscopic torque generated by rotating the body-fixed axis of a flywheel.

SECTION I. INTRODUCTION

The environment necessary for the life support of astronauts during extended space flights will probably have to include artificial gravity. During periods of coasting, this will be generated by continuous rotation of the space station around an axis that is sufficiently remote from the crew compartment to exclude extreme variations in the centrifugal forces within the compartment.

Our investigation will be limited to a station of cylindrical shape, since this is the geometry most likely to be used for early flights of long duration. As a further qualification, since the rotating cylinder is highly stable around its two axes of large moment of inertia, only the requirements for stability around the third axis, *i.e.*, the longitudinal axis, will be examined.

SECTION II. ANALYSIS

A. *The Undisturbed System*

In the absence of external torques, the angular impulse of the system remains constant. Let us assume that the angular impulse is aligned with the Z axis of the space-fixed reference coordinate system X, Y, Z (Figure 1). Using the transformation matrix from the reference coordinate system to the body-fixed coordinate system expressed in Euler angles ϕ, θ, ψ, we get the components of the angular impulse in the body-fixed coordinate system x, y, z (Figure 1):*

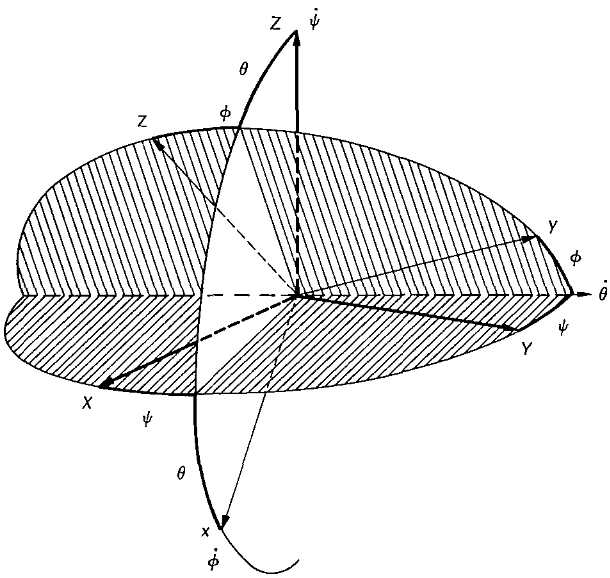

ψ, θ, ϕ as shown are positive angles.

Figure 1 — Euler Angles, Transformation from Reference to Body-Fixed Coordinate System

*This approach eliminates the drift problems that occur when Euler's moment equation is used for the analog simulation of torque-free rotational motion. Cf. Whittaker, E. T., *A Treatise on the Analytical Dynamics of Particles and Rigid Bodies*, New York, Dover (1944), pg. 144.

$$\begin{bmatrix} H_x \\ H_y \\ H_z \end{bmatrix} = \begin{bmatrix} \cos\psi\cos\theta & \sin\psi\cos\theta & -\sin\theta \\ \cos\psi\sin\theta\sin\phi - \sin\psi\cos\phi & \sin\psi\sin\theta\sin\phi + \cos\psi\cos\phi & \cos\theta\sin\phi \\ \cos\psi\sin\theta\cos\phi + \sin\psi\sin\phi & \sin\psi\sin\theta\cos\phi - \cos\psi\sin\phi & \cos\theta\cos\phi \end{bmatrix} \begin{bmatrix} 0 \\ 0 \\ H \end{bmatrix} \quad (1)^{**}$$

or

$$\begin{aligned} H_x &= -H\sin\theta \\ H_y &= H\cos\theta\sin\phi \\ H_z &= H\cos\theta\cos\phi \end{aligned} \quad (2)$$

The angular impulse is related to the angular velocity by the vector equation

$$\bar{H} = \tilde{I}\cdot\bar{\Omega} \quad (3)$$

The inertia tensor $\tilde{I}$ is given by a matrix

$$\tilde{I} = \begin{bmatrix} I_{xx} & -I_{xy} & -I_{xz} \\ -I_{yx} & I_{yy} & -I_{yz} \\ -I_{zx} & -I_{zy} & I_{zz} \end{bmatrix} \quad (4)$$

If there is no mass motion inside the space station, the components of the tensor are constant in the body-fixed coordinate system. Calling the components of the angular velocity in the body-fixed coordinate system p, q, r and using Equations (2), the vector equation (3) can be written in components

$$\begin{aligned} H_x &= I_x p - I_{xy} q - I_{xz} r = -H\sin\theta \\ H_y &= -I_{xy} p + I_y q - I_{yz} r = H\cos\theta\sin\phi \\ H_z &= -I_{xz} p - I_{yz} q + I_z r = H\cos\theta\cos\phi \end{aligned} \quad (5)$$

Using determinants, Equations (5) are solved for p, q, and r

$$p = \frac{D_1}{D}\,;\; q = \frac{D_2}{D}\,;\; r = \frac{D_3}{D}\,; \quad (6)$$

where

$$D = \begin{vmatrix} I_x & -I_{xy} & -I_{xz} \\ -I_{xy} & I_y & -I_{yz} \\ -I_{xz} & -I_{yz} & I_z \end{vmatrix}$$

$$D_1 = \begin{vmatrix} -H\sin\theta & -I_{xy} & -I_{xz} \\ H\cos\theta\sin\phi & I_y & -I_{yz} \\ H\cos\theta\cos\phi & -I_{yz} & I_z \end{vmatrix}$$

$$D_2 = \begin{vmatrix} I_x & -H\sin\theta & -I_{xz} \\ -I_{xy} & H\cos\theta\sin\phi & -I_{yz} \\ -I_{xz} & H\cos\theta\cos\phi & I_z \end{vmatrix}$$

$$D_3 = \begin{vmatrix} I_x & -I_{xy} & -H\sin\theta \\ -I_{xy} & I_y & H\cos\theta\sin\phi \\ -I_{xz} & -I_{yx} & H\cos\theta\cos\phi \end{vmatrix}$$

We now express the angular velocities in terms of gimbal angles and rates:

$$\begin{aligned} p &= \dot\phi - \dot\psi\sin\theta \\ q &= \dot\theta\cos\phi + \dot\psi\cos\theta\sin\phi \\ r &= -\dot\theta\sin\phi + \dot\psi\cos\theta\cos\phi \end{aligned} \quad (7)$$

Or, solving for $\dot\phi$, $\dot\theta$, and $\dot\psi$, we get

$$\begin{aligned} \dot\phi &= p + \dot\psi\sin\theta \\ \dot\theta &= q\cos\phi - r\sin\phi \\ \dot\psi\cos\theta &= q\sin\phi + r\cos\phi \end{aligned} \quad (8)$$

Finally, introducing (6) into (8), we get

$$\begin{aligned} D\dot\phi &= D_1 + (D_2\sin\phi + D_3\cos\phi)\tan\theta \\ D\dot\theta &= D_2\cos\phi - D_3\sin\phi \\ D\dot\psi\cos\theta &= D_2\sin\phi + D_3\cos\phi \end{aligned} \quad (9)$$

Equations (9) describe the attitude of a body with an angular impulse. This system of first-order differential equations can be simplified if we choose a particular body-fixed coordinate system that is aligned with the principal axes ζ, η, ξ. The inertia tensor $\tilde{I}$ can then be expressed by a diagonal matrix:

$$\tilde{I} = \begin{bmatrix} I_\xi & 0 & 0 \\ 0 & I_\eta & 0 \\ 0 & 0 & I_\zeta \end{bmatrix} \quad (10)$$

and equations (5) simplify to

$$\begin{aligned} \Omega_\xi I_\xi &= -H\sin\Theta \\ \Omega_\eta I_\eta &= H\cos\Theta\sin\Phi \\ \Omega_\zeta I_\zeta &= H\cos\Theta\cos\Phi \end{aligned} \quad (11)$$

Rewriting (8) in our new notation,

$$\begin{aligned} \dot\Theta &= \Omega_\eta\cos\Phi - \Omega_\zeta\sin\Psi \\ \dot\Phi &= \Omega_\xi + \dot\Psi\sin\Theta \\ \dot\Psi\cos\Theta &= \Omega_\eta\sin\Phi + \Omega_\zeta\cos\Phi \end{aligned} \quad (12)$$

Finally, we get

$$\dot\Theta = \frac{H}{2}\left(\frac{1}{I_\eta} - \frac{1}{I_\zeta}\right)\cos\Theta\sin 2\Phi$$

$$\dot\Psi = H\left(\frac{\sin^2\Phi}{I_\eta} + \frac{\cos^2\Phi}{I_\zeta}\right) \quad (13a)$$

$$\dot\Phi = H\left[-\frac{1}{I_\xi} + \left(\frac{\sin^2\Phi}{I_\eta} + \frac{\cos^2\Phi}{I_\zeta}\right)\right]\sin\Theta$$

**Cf. Fifer, Stanley, *Analogue Computation*, Vol. IV, New York, McGraw-Hill (1961), pg. 1091.

or, using

$$\cos^2 \Phi = \frac{1}{2} + \frac{1}{2}\cos 2\Phi$$

$$\sin^2 \Phi = \frac{1}{2} - \frac{1}{2}\cos 2\Phi$$

we get

$$\dot{\Psi} = \frac{H}{2}\left(\frac{1}{I_\eta} + \frac{1}{I_\zeta}\right) + \frac{H}{2}\left(\frac{1}{I_\zeta} - \frac{1}{I_\eta}\right)\cos 2\Phi \qquad (13b)$$

$$\dot{\Phi} = \frac{H}{2}\left[-\frac{2}{I_\xi} + \frac{1}{I_\eta} + \frac{1}{I_\zeta} + \left(\frac{1}{I_\zeta} - \frac{1}{I_\eta}\right)\cos 2\Phi\right]\sin\Theta \qquad (13c)$$

For rotational symmetry ($I_\eta = I_\zeta$)

$$\Theta,\ \dot{\Phi},\ \dot{\Psi} \text{ are constants}$$

and

$$\Omega_\xi = \text{constant}$$
$$\Omega_\eta = A \sin \Phi$$
$$\Omega_\zeta = A \cos \Phi$$

These equations describe the nutational motion of a cylinder of perfect rotational symmetry. The length axis is moving on a circular cone with constant angular and roll velocity—a well-known phenomenon.

Let us now consider the case of a body with near rotational symmetry around the length axis and small angle Θ:

$$I_\zeta - I_\eta = \Delta I \ll I_\zeta$$
$$\Theta \ll \Phi$$

and

$$\dot{\Theta} \approx \frac{1}{2}\frac{H \Delta I}{I_\zeta^2}\sin 2\Phi$$

$$\dot{\Phi} \approx -H\left(\frac{1}{I_\xi} - \frac{1}{I_\zeta}\right)\Theta$$

$$\dot{\Psi} \approx \frac{H}{I_\zeta}$$

Combining the first and the derivative of the second of these equations, we eliminate Θ and get

$$\ddot{\Phi} = -\frac{1}{2}\left(\frac{1}{I_\xi} - \frac{1}{I_\zeta}\right)\frac{H^2}{I_\zeta^2}\Delta I \sin 2\Phi \qquad (14)$$

i.e., the equation for the mathematical pendulum. For ΔI positive the rotation around the ζ-axis is stable, and for ΔI negative the rotation around the η-axis is stable, the period T increasing with decreasing ΔI.

B. *Effect of Mass Motion Within the System*

Next, how does a change in the mass distribution inside the station affect the motion of the station? The total angular impulse does not change because the mass motion is a result of internal forces. Nor does the center of mass move. But the origin of the body-fixed coordinate system does move and the inertia tensor changes. In addition, we must remember that the angular momentum varies with location. A mass close to the center of rotation has less angular momentum than a mass located farther out. Thus a mass that moves away from the center of rotation is accelerated, thereby slowing the part of the station it moves to. (This is equivalent to saying that a moving mass in a rotating system experiences the Coriolis force, which causes a change in the angular velocity of the station if it acts at an arm. See Figure 2.)

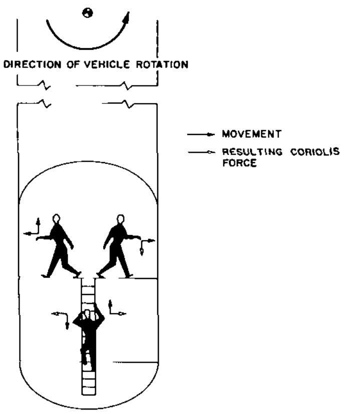

Figure 2 – Coriolis Forces Resulting from Mass Motion in Rotating Space Station

Let us assume that a mass m moves from $\bar{\rho}_o$ to $\bar{\rho}$ inside the station. Although the position vector of the center of mass in the space-fixed coordinate system does not change, the location $\bar{R}$ of the center of mass in the body-fixed coordinate system does move. Initially, we have

$$\sum_{m_i \neq m} m_i \bar{\rho}_i + m \bar{\rho}_o = 0$$

With m moved to $\bar{\rho}$ the center of gravity has moved to $\bar{R}$, given by

$$M \cdot \bar{R} = \sum_{m_i \neq m} m_i \bar{\rho}_i + m \bar{\rho}$$

$$= m \bar{\rho} - m \bar{\rho}_o \qquad (15)$$

$$\bar{R} = \frac{m}{M}(\bar{\rho} - \bar{\rho}_o)$$

where M is the total mass of the system.

The angular impulse $\bar{H}$, which remains unchanged, is given by

$$\bar{H} = \sum_{\text{all } m} m_i \bar{r}_i \times \bar{v}_i$$

with $\bar{r}_i$ the position vector of m_i and $\bar{v}_i$ the velocity of m_i (relative to the center of mass) measured in space-fixed coordinates.

We write the equation for the angular impulse in body-fixed coordinates:

$$\bar{r}_i = \bar{\rho}_i - \bar{R}$$

$$\bar{v}_i = \frac{d}{dt}(\bar{r}_i) = \dot{\bar{r}}_i + \bar{\Omega} \times \bar{r}_i$$

$$= \dot{\bar{\rho}}_i - \dot{\bar{R}} + \bar{\Omega} \times (\bar{\rho}_i - \bar{R})$$

$$\bar{H} = \sum m_i (\bar{\rho}_i - \bar{R}) \times (\dot{\bar{\rho}}_i - \dot{\bar{R}}) + \sum m_i (\bar{\rho}_i - \bar{R}) \times \bar{\Omega} \times (\bar{\rho}_i - \bar{R})$$

Using the formula $\bar{a} \times (\bar{b} \times \bar{c}) = \bar{b}(\bar{a}\cdot\bar{c}) - \bar{c}(\bar{a}\cdot\bar{b})$, we get

$$\bar{H} = \sum m_i(\bar{\rho}_i - \bar{R}) \times \dot{\bar{\rho}}_i - \sum m_i(\bar{\rho}_i - \bar{R}) \times \dot{\bar{R}} + \bar{\Omega} \sum m_i(\bar{\rho}_i - \bar{R})^2 - \sum m_i(\bar{\rho}_i - \bar{R}) \cdot [\bar{\Omega} \cdot (\bar{\rho}_i - \bar{R})] \quad (16)$$

The first two terms show the effect of the mass motion; the last two terms, which depend only on the mass distribution, must correspond with Equation (3). Evaluating the first two terms further, we note that because $\dot{\bar{\rho}}_i = 0$ for all m_i except the moving mass m,

$$\sum m_i(\bar{\rho}_i - \bar{R}) \times \dot{\bar{\rho}}_i = m(\bar{\rho} - \bar{R}) \times \dot{\bar{\rho}}$$

and, according to the definition of $\bar{R}$,

$$\sum m_i(\bar{\rho}_i - \bar{R}) = 0$$

Therefore the second term equals zero:

$$\sum m_i(\bar{\rho}_i - \bar{R}) \times \dot{\bar{R}} = 0$$

The equation for the angular impulse is now

$$\bar{H} = m(\bar{\rho} - \bar{R}) \times \dot{\bar{\rho}} + \tilde{I}\cdot\bar{\Omega} \quad (17)$$

The x component of $\tilde{I}\cdot\bar{\Omega}$ (see Equation 16) is given by

$$(\tilde{I}\cdot\bar{\Omega})_x = p\sum m_i[(x_i - X)^2 + (y_i - Y)^2 + (z_i - Z)^2] - p\sum m_i(x_i - X)^2 - q\sum m_i(x_i - X)(y_i - Y) - r\sum m_i(x_i - X)(z_i - Z)$$

$$= p\sum m_i[(y_i - Y)^2 + (z_i - Z)^2] - q\sum m_i(x_i - X)(y_i - Y) - r\sum m_i(x_i - X)(z_i - Z)$$

and the other components of $\tilde{I}\cdot\bar{\Omega}$ have the corresponding form. We use these equations to evaluate the inertia tensor $\tilde{I}$:

$$Ix = \sum m_i[(y_i - Y)^2 + (z_i - Z)^2]$$

$$= \sum m_i(y_i^2 + z_i^2) - 2Y\sum m_i Y_i - 2Z\sum m_i z_i + M(Y^2 + Z^2)$$

$$= I_{x,o} - m(y_o^2 + z_o^2) + m(y^2 + z^2) - 2Ym(y - y_o) - 2Zm(z - z_o) + M(Y^2 + Z^2)$$

and (see Equation 15)

$$I_x = I_{x,o} + m(y^2 - y_o^2) + m(z^2 - z_o^2) - \frac{m^2}{M}(y - y_o)^2 - \frac{m^2}{M}(z - z_o)^2 \quad (18a)$$

where $I_{x,o}$ is the x-component of I before the mass m is moved from ρ to ρ_o.
Since the body axes are the principal axes for $\rho = \rho_o$, we get

$$I_{xy} = m(xy - x_o y_o) - \frac{m^2}{M}(x - x_o)(y - y_o) \quad (18b)$$

Similarly, we get

$$I_y = I_{y,o} + m(x^2 - x_o^2) + m(z^2 - z_o^2) - \frac{m^2}{M}(x - x_o)^2 - \frac{m^2}{M}(z - z_o)^2 \quad (18c)$$

$$I_z = I_{z,o} + m(x^2 - x_o^2) + m(y^2 - y_o^2) - \frac{m^2}{M}(x - x_o)^2 - \frac{m^2}{M}(y - y_o)^2 \quad (18d)$$

$$I_{xz} = m(xz - x_o z_o) - \frac{m^2}{M}(x - x_o)(z - z_o) \quad (18e)$$

$$I_{yz} = m(yz - y_o z_o) - \frac{m^2}{M}(y - y_o)(z - z_o) \quad (18f)$$

where $I_{y,o}$ and $I_{z,o}$ are quantities corresponding to $I_{x,o}$.
Equations (17) and (18) describe the dynamics of a rotating space station with no external torques.

For our numerical evaluation of Equations (15), (17), and (18), we have used a model of a space station similar to one proposed in a study conducted by the Propulsion and Vehicle Engineering Laboratory, Marshall Space Flight Center, at the request of the MSFC Future Projects Office (Figure 3). The station is nearly cylindrical and rotates around its axis of maximum moment of inertia. The rate of rotation, Ω, is 0.628 rad/sec and the crew compartment extends 12 to 18 meters from the center of rotation. The re-

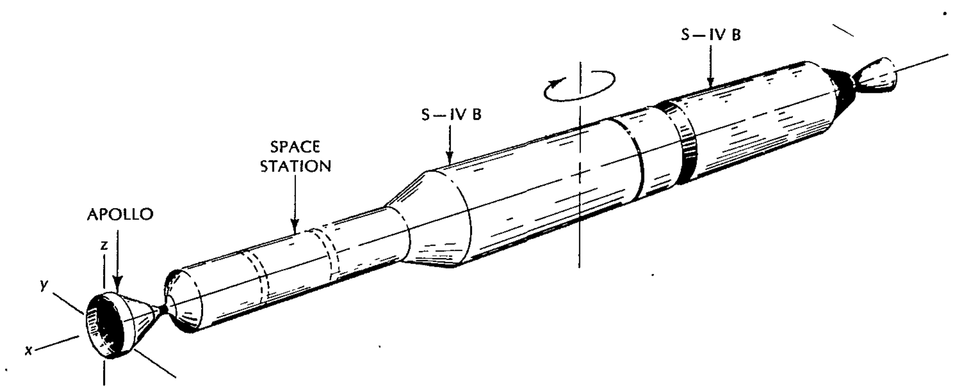

Figure 3 — Model of Rotating Space Station

sulting artificial gravity, $\Omega^2 \cdot r$, ranges from 0.48g to 0.72g. Three astronauts weighing 90 kilograms each are free to move about in this area. The maximum moment of inertia, I_z, is 6,000,000 kg m^2. The moment of inertia around the length axis, I_x, is 112,000 kg m^2.

Several different mass motions were studied. Our study showed that a station with rotational symmetry around the length axis responds to mass disturbances with large roll motions. This is demonstrated on Figure 4, which shows the results of a digital evaluation. A continuous roll motion is produced in response to a mass motion from $x = 15$m, $z = 0$ to $x = 15$m, $z = 1.8$m. The deflection in θ is negligible. (The deflection in θ consists of a component proportional to cos ϕ and, according to Equation (13c), superimposed on this a component proportional to $\dot{\phi}$. The component proportional to cos ϕ is caused by the angle between the principal axis ξ and the body axis x.) The mass motion converts the z-axis into an axis of intermediate moment of inertia, the rotation around this axis is unstable, and because the motion (the distance of m from the center of rotation increases) introduces a small positive initial roll velocity, the roll motion is continuous.

But even as little as 0.2% asymmetry is sufficient (for the model used in our numerical evaluation) to insure that the roll deflection in response to a single motion is limited to less than 10°. However, because of the absence of damping, whether or not a new mass motion will increase or decrease an existing oscillation depends on the timing of the new mass motion. (See the discussion of cancellation of roll by motion of the astronauts, page 34.)

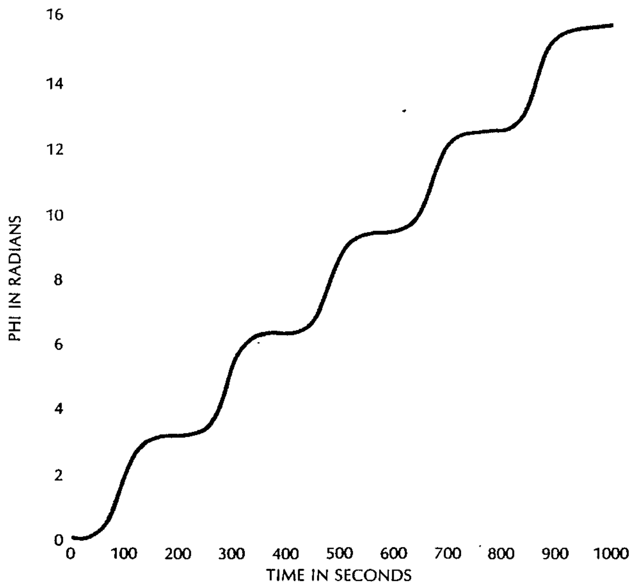

Figure 4a — ϕ Response of Station
to Mass Motion from $x = 15$m, $z = 0$ to $x = 15$m, $z = 1.8$m
(Given Rotational Symmetry Around Length Axis)

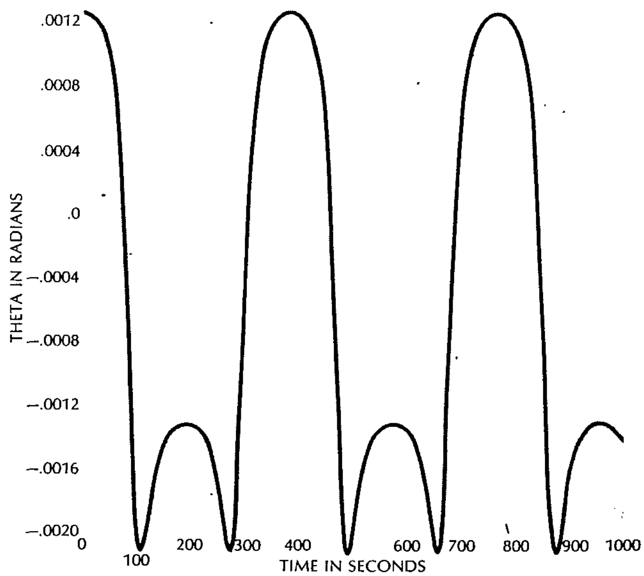

Figure 4b — θ Response of Station
to Mass Motion from $x = 15$m, $z = 0$ to $x = 15$m, $z = 1.8$m
(Given Rotational Symmetry Around Length Axis)

Another disturbance that can be considered is the effect of rotating machinery (generators, pumps, etc.) on board the station. We modify Equation (17) to include the effect of rotating machinery with body-fixed axes:

$$\overline{H} = m(\overline{\rho} - \overline{R}) \times \dot{\overline{\rho}} + \widetilde{I} \cdot \overline{\Omega} + \overline{h} \qquad (19)$$

where $\overline{h}$ is the angular impulse of the rotating machinery. Written in components, Equation (19) becomes

$$-H \sin\theta = h_x + p\, I_x - q\, I_{xy} - r\, I_{xz} + m\,[(y - Y)\dot{z} - (z - Z)\dot{y}]$$

$$H \cos\theta \sin\Phi = h_y - p\, I_{xy} + q\, I_y - r\, I_{yz} + m\,[(z - Z)\,\dot{x} - (x - X)\dot{z}]$$

$$H \cos\theta \cos\Phi = h_z - p\, I_{xz} - q\, I_{yz} + r\, I_z + m\,[(x - X)\,\dot{y} - (y - Y)\dot{x}]$$

We see from these equations that flywheels can enforce the correct attitude in the steady state, in spite of mass displacements.

In the steady state, with p, q, $\dot{x}$, $\dot{y}$, and $\dot{z} = 0$, ϕ and θ can be reduced to zero if

$$h_x = r\, I_{xz}$$

$$h_y = r\, I_{yz}$$

We can determine the required angular impulses to do this for the maximum possible values of I_{xz} and I_{yz}:

$$I_{xz} = mxz = 270\text{kg} \cdot 18\text{m} \cdot 1.8\text{m} = 8{,}750\text{kg m}^2$$

$$I_{yz} = myz = 270\text{kg} \cdot 1.27\text{m} \cdot 1.27\text{m} = 435\text{kg m}^2$$

Because the roll deflection is considerably larger than the pitch deflection, it is more important to reduce roll. Fortunately, this requires a twenty times smaller angular impulse. Moreover, because a deflection in the roll orientation is less disturbing to the astronauts than a roll oscillation, only methods of limiting roll oscillation were studied. Two methods were studied in detail: controlled motion of the astronauts and automatic control by flywheels.

To simplify our analysis of the effect of rotating machinery with body-fixed axes, we shall assume that the body-fixed axes are the principal axes and that the astronauts are at rest. Equations (19) then become

$$-H \sin\theta = h_x + p\, I_x$$

$$H \cos\theta \sin\phi = h_y + q\, I_y$$

$$H \cos\theta \cos\phi = h_z + r\, I_z$$

The magnitude of h_x that can be tolerated is determined by the transients it introduces into roll during starting and stopping.

We can estimate the initial roll velocity caused by a fast start (assuming that $\theta = 0$ initially) from

$$I_x p + h_x = 0 = h_x + I_x \dot{\phi}_o$$

If we limit the roll deflection to a maximum of 0.1 rad, the roll oscillation will be approximately sinusoidal, with the relation between the maximum angular velocity and the angular deflection given by

$$\phi_m = \frac{T}{2\pi} \dot{\phi}_o$$

It follows that

$$|h_x| < \frac{I_x \cdot 2\pi}{T} \cdot 0.1 \text{ rad} = 1850\text{kg m}^2 \text{ sec}^{-1}$$

This angular impulse causes a deflection in θ after the roll oscillation is damped out:

$$\theta = -\frac{h_x}{H} = \frac{1850}{6{,}000{,}000 \cdot 0.628}$$

$$= -0.5 \cdot 10^{-3} \text{ rad}$$

But, because of their small size, θ and $\dot{\theta}$ can be neglected, and we get for the components of Ω:

$$q = \dot{\psi} \cos\theta \sin\phi \qquad r = \dot{\psi} \cos\theta \cos\phi$$

Using these expressions, we get

$$h_z = (H - \dot{\psi}\, I_z) \cos\theta \cos\phi$$

or

$$\dot{\psi} \approx \frac{H - h_z}{I_z}$$

Thus, because H is very large, the change in $\dot{\psi}$ resulting from rotating machinery with its axis parallel to z can be neglected.

Finally, for h_y, we get

$$h_y \approx H\left(1 - \frac{I_y}{I_z}\right) \cos\theta \sin\phi$$

Hence an angular impulse h_y causes a steady-state deflection in ϕ. Imposing the same limit on the steady-state deflection as we did on the roll oscillation, we get

$$h_y < H\left(1 - \frac{I_y}{I_z}\right) \cdot 0.1$$

$$< 6{,}000{,}000 \cdot 0.002 \cdot 0.628 \cdot 0.1$$

$$< 750 \text{ kg m}^2 \text{ sec}^{-1}$$

In sum, then, rotating machinery interferes least with the dynamics of the rotating station when its axis is aligned with the z-axis of the station.

SECTION III. NUMERICAL EVALUATION

A. *The Analog Computer Program*

To study the behavior of Equation (19), we programmed it on an analog computer. Mechanization in the most general manner had to include the following: the variation in the nine components of the inertia tensor resulting from changes in the mass distribution, the angular impulse of the moving mass inside the station, and the relation between the components of the angular impulse (in the body-fixed coordinate system) and the Euler angle rates. Seven multipliers, with 35 products, and two resolvers were required.

By various linearizations and approximations, this requirement was reduced to four multipliers, with 11 products. The largest error (7% in the worst case) was introduced into the factor of ϕ by the replacement of $1 - I_y/I_z$ with $1 - I_{y,o}/I_{z,o}$.

The following simplifying assumptions were made: that $m << M$, that the position of m in the undisturbed system is at $y_o, z_o = 0$, that changes in I_x, I_y, I_z resulting from mass displacements can be neglected, and that small angle approximations will have no significant effect on the results. We therefore get

$$I_{xy} \approx mxy;\ I_{yz} \approx myz;\ I_{zx} \approx mxz$$

$$p \approx \dot{\phi} - \dot{\psi}\theta;\ q \approx \dot{\theta} + \dot{\psi}\phi;\ r \approx \dot{\psi} \approx \frac{H}{I_z}$$

$$I_x\dot{\phi} \approx -H\left(1 - \frac{I_x}{I_z}\right)\dot{\theta} + mxy\,\dot{\theta} + m\frac{H}{I_z}xy\,\phi + m\frac{H}{I_z}xz + m(\dot{y}z - \dot{z}y) - h_x$$

$$I_y\dot{\theta} \approx H\left(1 - \frac{I_y}{I_z}\right)\phi + mxy\,\dot{\phi} - m\frac{H}{I_z}xy\,\theta + m\frac{H}{I_z}yz + m(x\dot{z} - z\dot{x}) - h_y \qquad (20)$$

The analog computer program is shown in Figure 5.

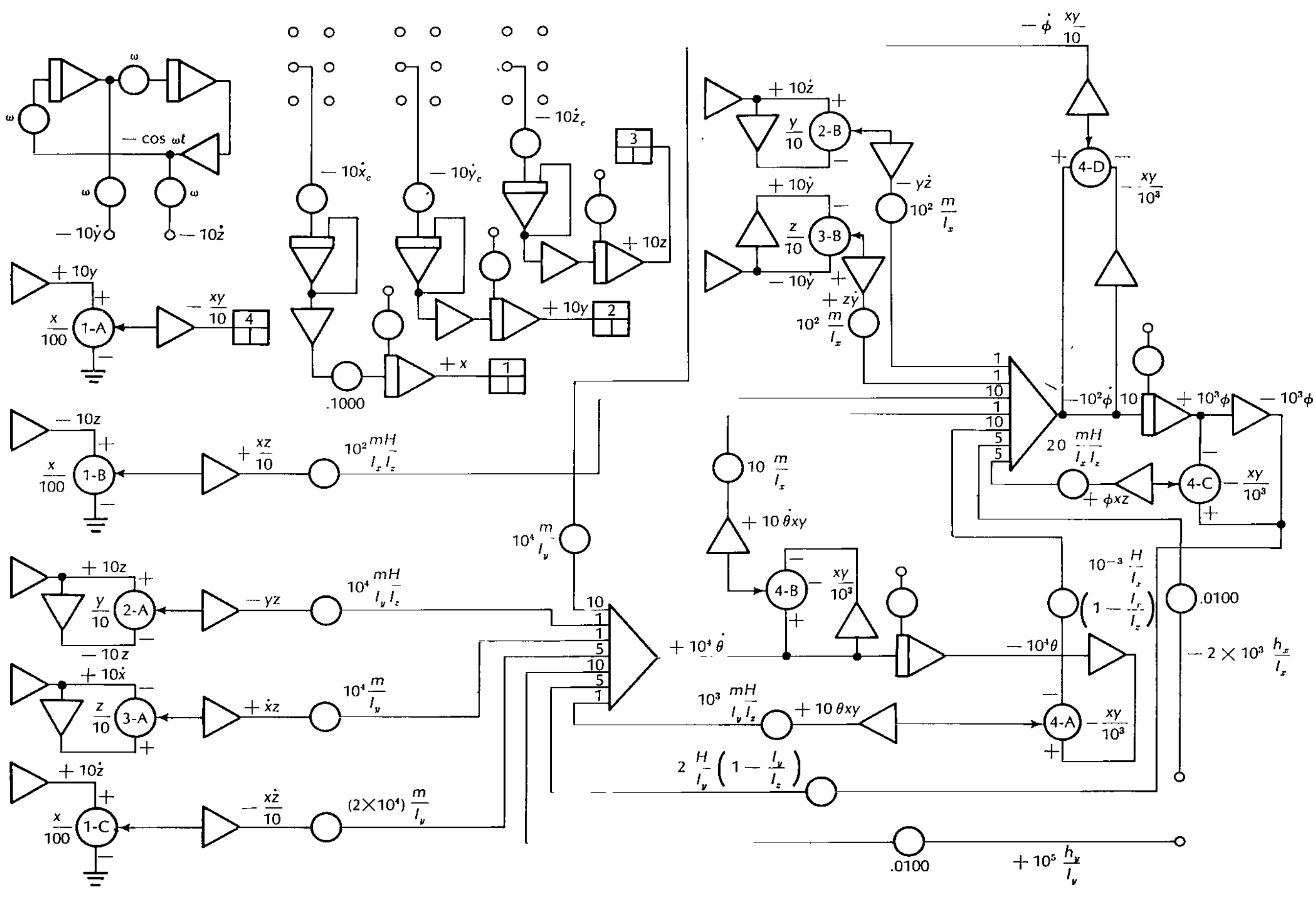

Figure 5 – Basic Analog Computer Program

The effect of a mass displacement depends on the path and on the schedule of the displacement. Figure 6 shows the response of the station to the motion of three astronauts (3·90 kg = 270kg) from (12m, 0, 0) to (18m, 0, 1.8m) along three different paths:

Path I. From (12m, 0, 0) to (18m, 0, 0) and then to (18m, 0, 1.8m)

Path II. From (12m, 0, 0) to (18m, 0, 1.8m) and then to (18m, 0, 1.8m)

Path III. From (12m, 0, 0) to (12m, 0, 1.8m) and then to (18m, 0, 1.8m)

Check runs on a digital computer show good agreement, indicating that the approximations used have no significant effect on the results. It follows from Equation (13a) that the pitch amplitude is 0.007 of the roll amplitude. This too is in agreement with the computer results. The steady-state pitch deflection can be determined from Equation (E) of the Appendix, where the orientation of the principal axes of the space station relative to the body-fixed axes is described.

B. *Effects of Astronauts' Motion*

The walking speed was assumed to be 0.9 m/sec. To simulate changes in velocity realistically, a first-order lag with a time constant of one second was added to the velocity term.

Motion in the *yz* plane, for example the motion of three astronauts from (18m, 0, 0) to (18m, 1.2m, 1.2m), changes the direction of the principal axes η, ζ relative to the body axes and causes a roll oscillation, but the deflection in this case is only 2°. If this transfer occurs in two phases, for example from (18m, 0, 0) to (18m, 0, 1.2m) and then to (18m, 1.2m, 1.2m), a small initial roll velocity ($+2.5 \cdot 10^{-3}$ rad/sec) is introduced in the second phase. The same two-phase transfer in a different sequence, *i.e.*, from (18m, 0, 0) to (18m, 1.2m, 0) and then to (18m, 1.2m, 1.2m), produces a small initial roll velocity of the opposite sign.

Because starting and stopping occur in time intervals that are small compared with the period of the oscillation, the effect of these on the roll amplitude can be neglected (Figure 7a-c).

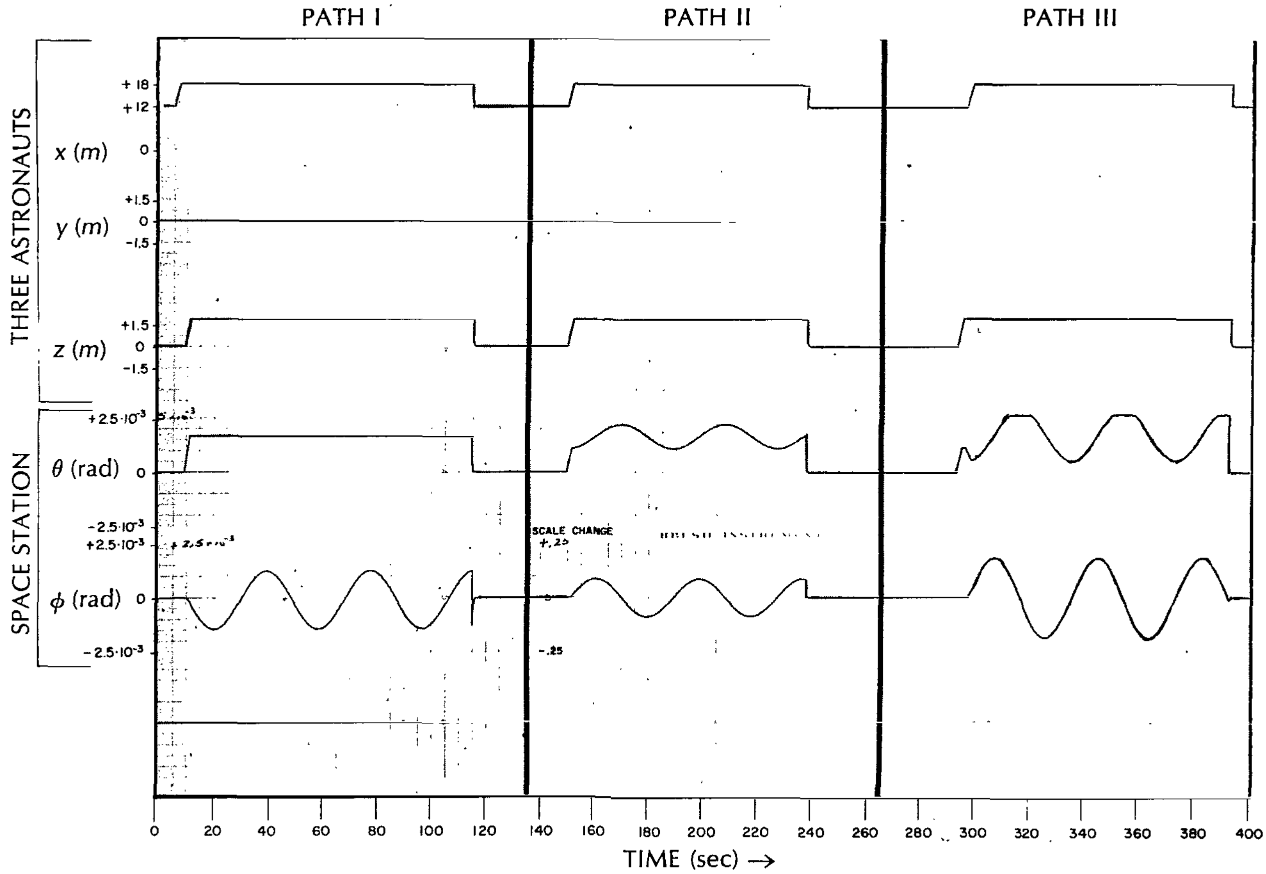

Figure 6 – Response of Station to Motion in Unison of Three Astronauts from (12m, 0, 0) to 18m, 0, 1.8m) along Three Different Paths. (Note 100-to-One Scale Change in ϕ between Path I and Paths II and III.)

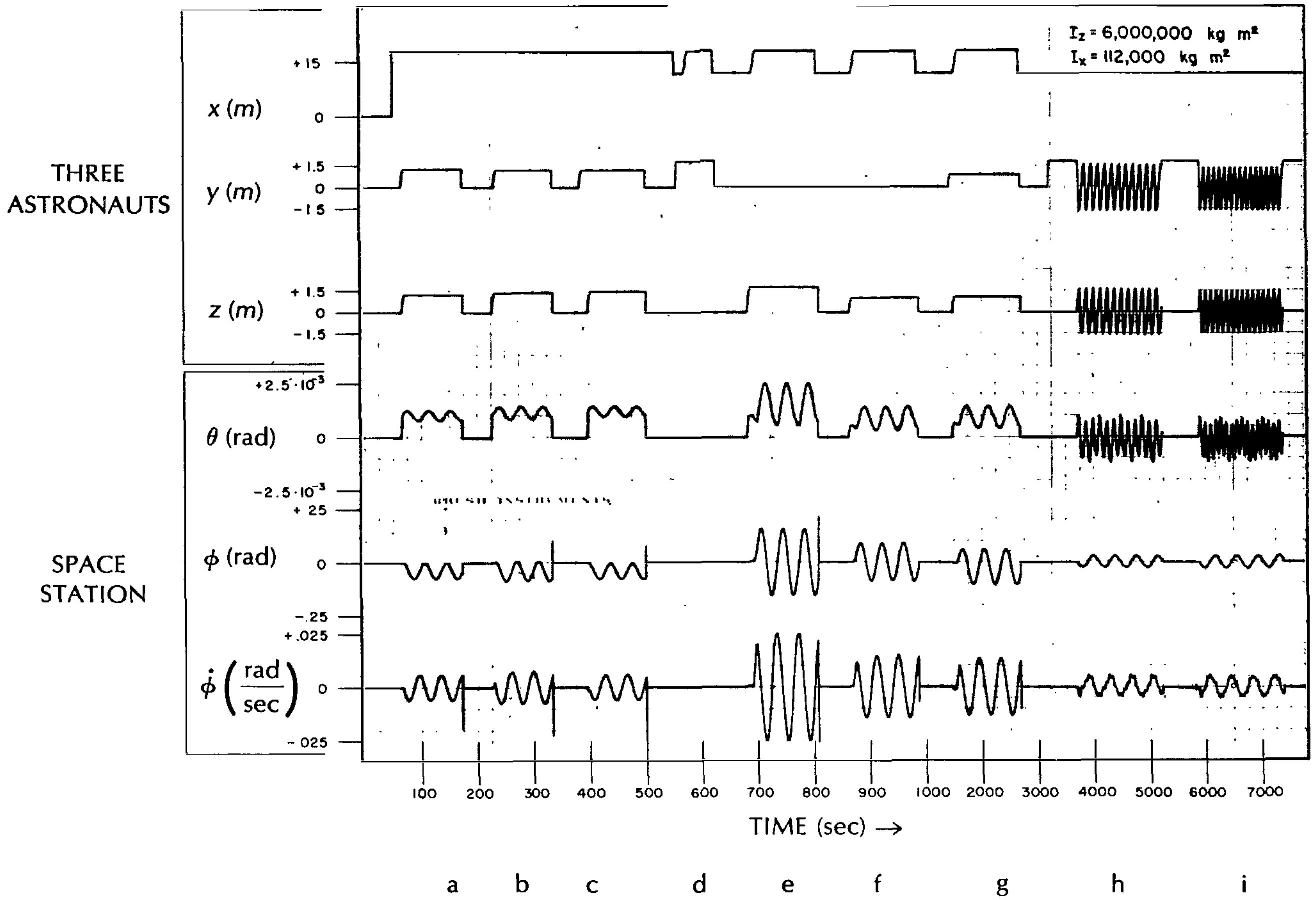

Figure 7 — Response of Station to Motion in Unison of Three Astronauts (a-c) in yz Plane ($x = 18$m), (c, d) in xy Plane ($z = 0$), (e-g) Parallel to but Not Along x Axis, (h, i) in Circle in yz Plane ($x = 15$m)

Motion in the xy plane ($z = 0$) causes no roll, as can be seen in Figure 7c, d. The ladder for going from a lower to an upper deck of the space station should therefore be located in the xy plane ($z = 0$).

Motion parallel to, but not along, the x-axis (constant $z \neq 0$) introduces large roll disturbances, mainly because of the change in angular momentum with distance from the center of rotation. The transfer of this momentum to the roll axis depends only on z, *i.e.*, the torque generated by the Coriolis force (Figure 7e-g).

Walking in a circle in the yz plane (Figure 7h, i) introduces two disturbances: the attitude of the principal axes relative to the body axes is varied, and an angular roll impulse is introduced. The first disturbance has a period corresponding to the time it takes to walk around half the circumference of the cylindrical station. Its effect can be seen in $\dot{\phi}$. The second disturbance is the reaction of the station to the initiation of circular motion by the astronauts. The initial roll velocity that results is given by

$$I_x \dot{\phi}_o = m\rho \cdot v = 270\text{kg} \cdot 1.8\text{m} \cdot 0.9 \text{ m/sec}$$

The amplitude of the resultant roll ($T =$ the period of the roll motion) is

$$\phi = \frac{\dot{\phi}_o \cdot T}{2\pi} = 24 \cdot 10^{-3} \text{ rad}$$

All these disturbances are moderate. The roll angle never exceeds 10°. However, whether the roll of the space station is increased or decreased depends on the phase of the recurrence of a disturbance.

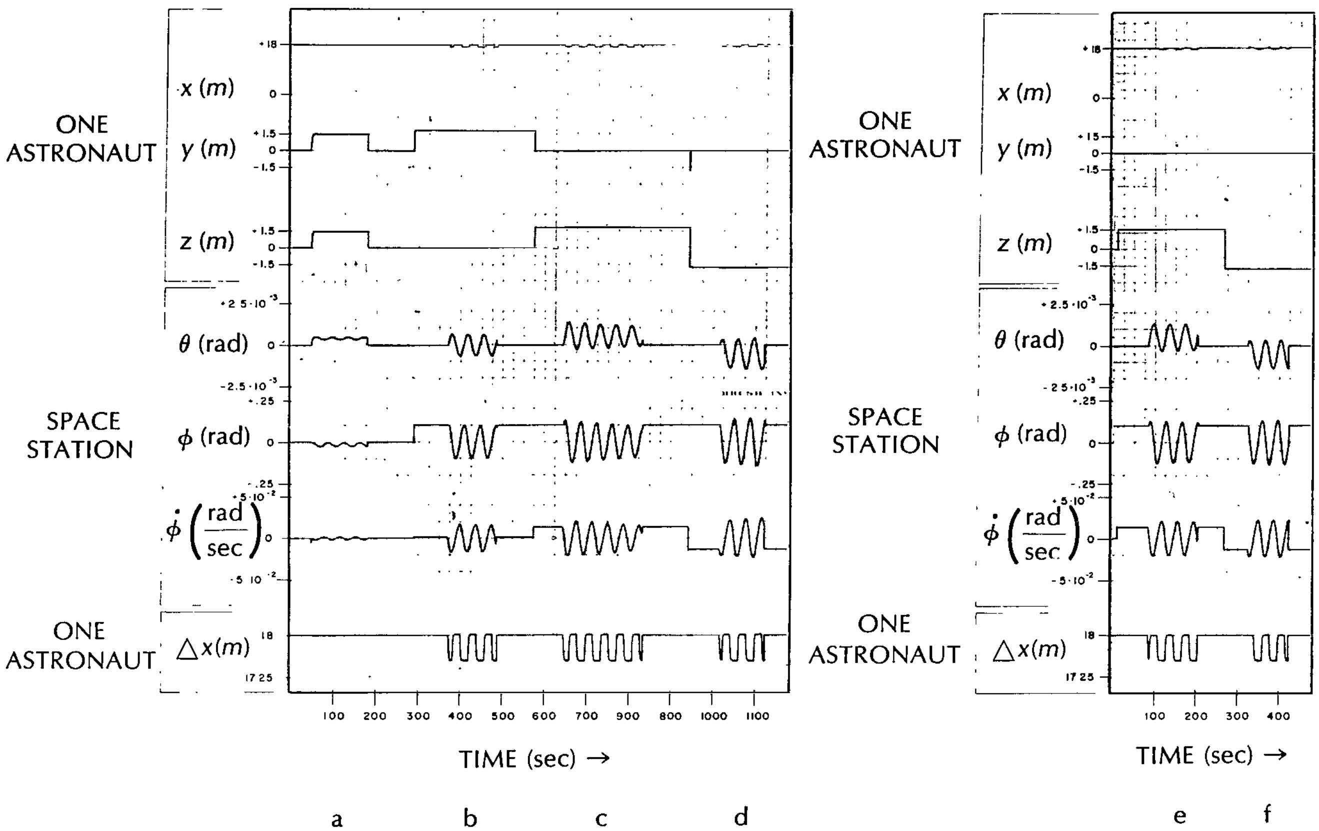

Figure 8 – Effect of One Astronaut Moving in x Direction Synchronously with Roll: (a) Check Run, Repeat of Figure 6, (b) Roll Unaffected by Motion in xy Plane ($z = 0$), (c) Damping of roll ($z > 0$), (d) Augmentation of Roll ($z < 0$), (e, f) Roll Unaffected by Motion in Phase with $\dot{\phi}$

Figure 8 shows the effect of one astronaut moving in the *x* direction synchronously with a roll oscillation. Whether the effect is one of buildup or of decay depends on the phase relation. Hence it should be feasible to use the astronauts for corrective action to counteract roll of the space station. Figure 8b shows again (as did Figure 7c, d) that motion in the *xy* plane ($z = 0$) does not affect roll. Figure 8c shows a damping effect ($z > 0$); Figure 8d shows an augmentation ($z < 0$) for motion in the *x* direction in phase with ϕ; Figure 8e, *f* shows that motion in the *x* direction in phase with $\dot{\phi}$ has no effect.

A more effective and convenient way to reduce a roll oscillation is shown on Figure 9. Here the motion is parallel to, but not along, the *y*-axis (constant $z \neq 0$) or parallel to, but not along, the *z*-axis (constant $y \neq 0$) in phase with the roll velocity.* The same motion in the opposite phase causes a buildup.

Very little has to be added to the basic analog program to simulate motion of an astronaut synchronized with a roll oscillation of the station. The additions to the basic program are shown on Figure 10. With Integrator 8 (Figure 10) providing an adjustable first-order time lag, Amplifier 9 generates the sign of $\dot{\phi}$ or, with S1 closed, the sign of *p*. The bridge limiter inserts a threshold, so that corrective action is taken by the astronaut only if roll exceeds a certain limit. The $\dot{x}_c$, $\dot{y}_c$, and $\dot{z}_c$ commands are connected to their integrators over a pair of relay switches that keep the resultant motion within preset limits. For example, the astronaut cannot move beyond the wall of the space station, *i. e.*, *y* and *z* must always be less than 1.8m.

*Measured as $\dot{\phi}$, *i. e.*, as the gimbal rate of the inertial platform, or as p by a rate gyro mounted on the frame of the space station

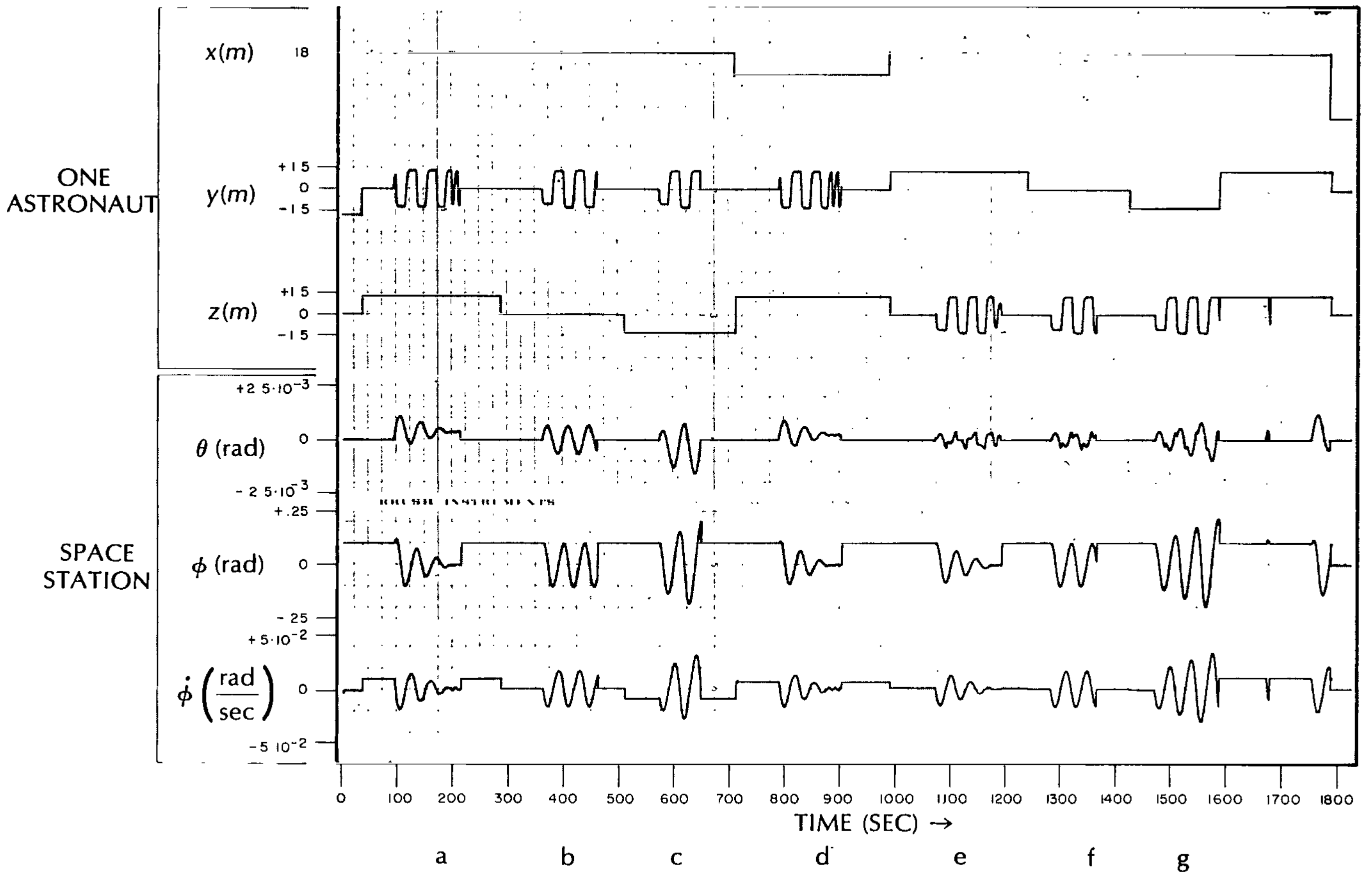

Figure 9 – Correction of Initial Roll Disturbance by Controlled Motion of One Astronaut in yz Plane

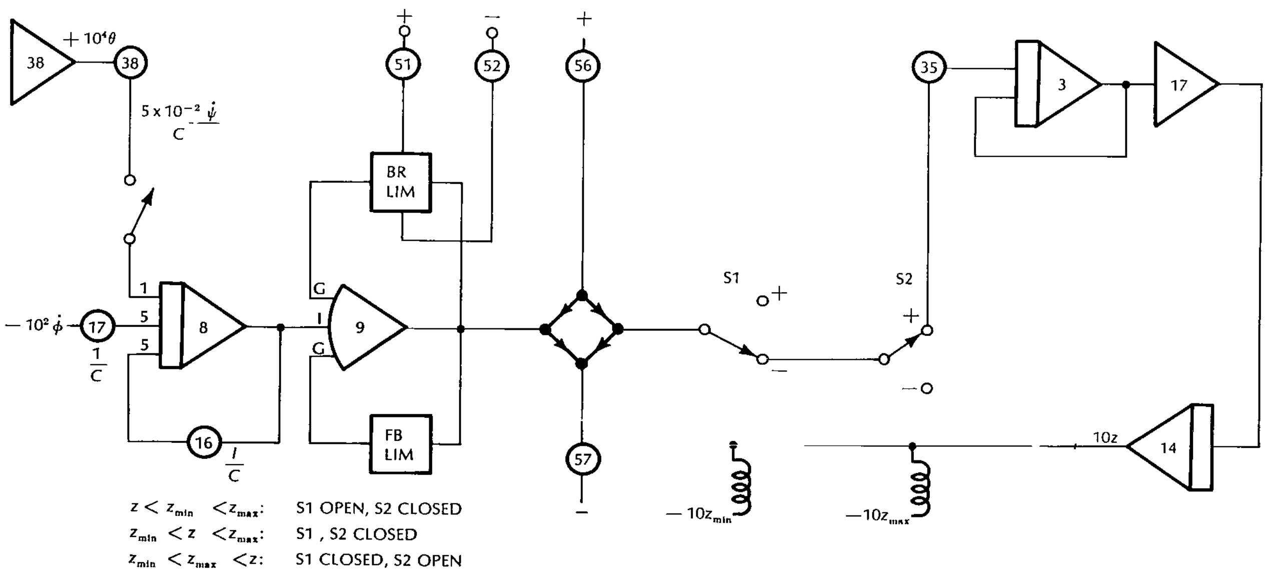

Figure 10 – Computer Program: Motion of Astronaut Synchronized with Roll Oscillation of Station

C. *Automatic Control of Station's Roll Motion*

As already mentioned, properly controlled variations in flywheel rates could be used to damp out roll oscillations. We shall first consider the effect of a flywheel with its axis parallel to the x-axis.

For simplicity, we assume that $I_{xy}, I_{yz}, I_{zx} = 0$ and that the astronauts are not moving. The station has a roll oscillation introduced by some previous disturbance. We use small angle approximations and Equation (19) becomes, with $I_z - I_y = \Delta I$ and $I_z >> \Delta I$,

$$-H\theta \approx h_x + pI_x \qquad p \approx \dot{\phi} - \dot{\psi}\theta$$

$$H\phi \approx qI_y \qquad q \approx \dot{\theta} + \dot{\psi}\phi$$

$$H \approx rI_z \qquad r \approx \dot{\psi}$$

Thus

$$\ddot{\phi} \approx -H\left(\frac{1}{I_x} - \frac{1}{I_z}\right)\dot{\theta} - \frac{\dot{h}_x}{I_x}$$

$$\dot{\theta} \approx \frac{\Delta I}{I_z} r\phi$$

and

$$\ddot{\phi} \approx -\frac{\Delta I}{I_x} r^2\phi - \frac{\dot{h}_x}{I_x} \qquad (21)$$

This equation shows that only a rate of the angular impulse of the flywheel, $\dot{h}_x$, generates a torque. Thus if $\dot{h}_x$ can be varied synchronously with $\dot{\phi}$, the roll oscillation of the station can be damped. But $\dot{h}_x$ cannot be used to counteract a steady-state deflection in ϕ caused by I_{yz}. However, as Figure 7a shows, the largest possible steady-state deflection due to I_{yz} is only 2°.

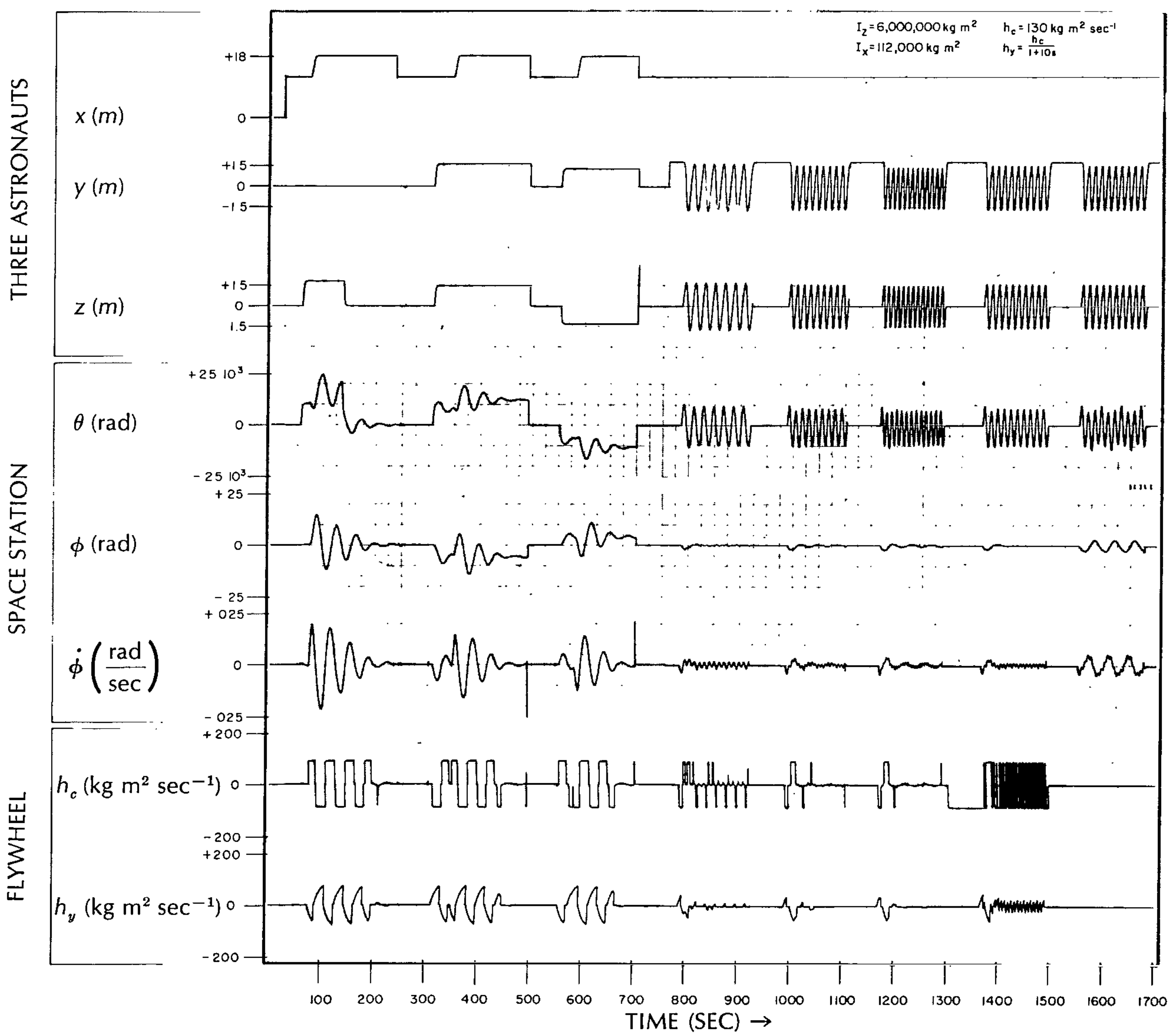

Figure 11 – Correction of Initial Roll Disturbance by Flywheel Control System

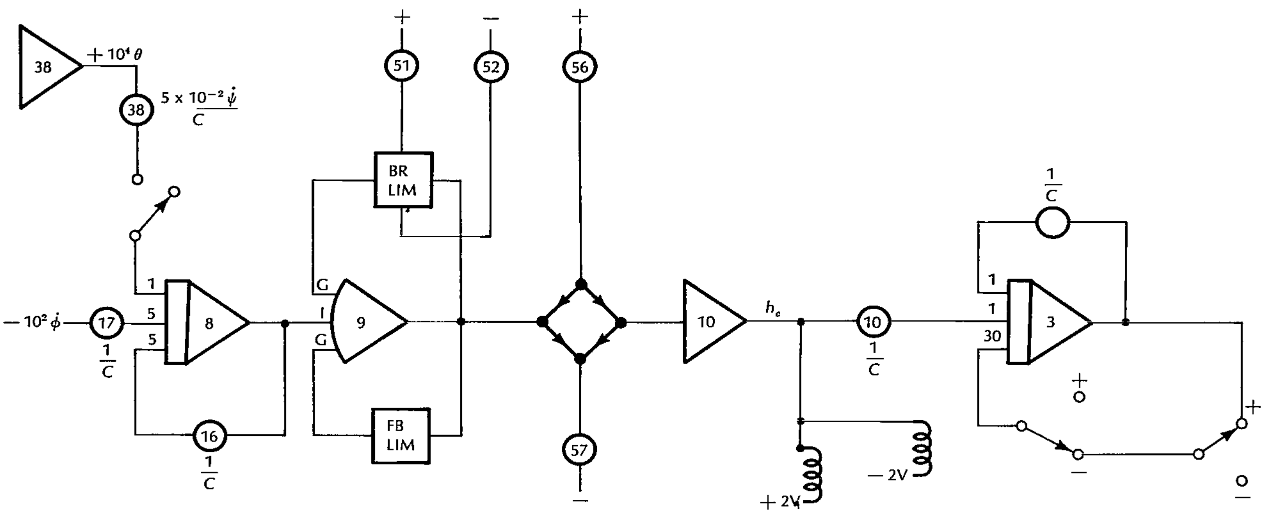

Figure 12 – Computer Program: Synchronous Motion of Flywheel for Automatic Roll Control

Another possibility is to use a flywheel with its axis parallel to the y-axis. Using the same approximations, we get

$$\ddot{\phi} \approx -\frac{\Delta I}{I_x} r^2 \phi + r \frac{h_y}{I_x} \qquad (22)$$

We now get a damped roll oscillation if the angular impulse of the flywheel, h_y, is varied synchronously with $-\dot{\phi}$. Comparing Equations (21) and (22), we can see that for an equal damping effect

$$r h_y = \dot{h}_x$$

An effective schedule for h was found to be a linear increase with time followed by an instantaneous braking action (Figure 11). For this schedule $\dot{h}_x$ is related to $h_{x_{max}}$ as follows (T = the roll period):

$$h_{x_{max}} = \dot{h}_x \cdot \frac{T}{2} = 19\dot{h}_x = 19 \cdot 0.628 h_{y_{max}}$$

$$= 12 h_{y_{max}}$$

Control by varying h_y thus turns out to be considerably more effective.

The additions to the basic analog program to simulate such a control system are shown on Figure 12. The discharge of Integrator 3 (Figure 12) through the two relay switches occurs in the intervals when the angular impulse of the flywheel, h_c on Figure 12, approaches zero (adjusted by potentiometers 51 and 52).

The performance of the flywheel control system is illustrated in Figure 11. No phase adjustments were made to optimize the control.

The simulation assumes that the flywheel* is driven by a motor with a combined time constant of 10 seconds. (Therefore h_y does not remain constant, as was assumed above, but decays during the cycle.) The voltage applied to the motor is constant; only the polarity is controlled. Brakes are applied before the voltage is reversed. Thus

$$E = \text{const. sign } \dot{\phi} = c \cdot h_c$$

$$h_y = \frac{h_c}{1 + 10s}$$

The maximum required power, P, is half the maximum torque multiplied by half the maximum angular rate, *i.e.*,

$$P_{max} = \frac{1}{4} \dot{h}_{max} \cdot \frac{h_{max}}{I_F}$$

With $I_F = 2\text{kg m}^2$ and $h_c = 100$ lb ft sec^{-1} $= 130\text{kg m}^2\ \text{sec}^{-1}$, we get

$$P_{max} = \frac{1}{4} \frac{130}{10} \cdot \frac{130}{2}$$

$$= 211 \text{ watts}$$

The maximum angular rate is therefore

$$w = \frac{130}{2} = 65 \text{ rad/sec}$$

$$= 620 \text{ rpm}$$

*A hydraulic system with circulating pump and valves could well be another feasible solution to the control system problem.

Or, rather than building up an angular impulse and then wasting the stored energy by braking, we can use a gimbal-mounted gyro with its axis aligned initially with the z-axis (Figure 13). The required angular impulse, h_y, is generated by rotating the gimbal (its axis is parallel to the x-axis) through an angle δ:

$$h_y = -I_s \Omega_s \sin \delta$$

($I_s \cdot \Omega_s$ is the angular impulse of the spinning gyro.)

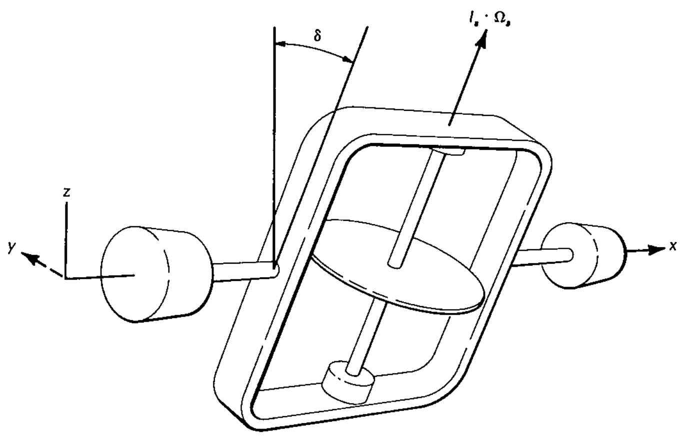

Figure 13 – Stabilization by a Gyro

The other two components of the angular impulse generated by this rotation are

$$h_x = I_{G,x} \dot{\delta}$$
$$h_z = I_s \Omega_s \cos \delta$$

($I_{G,x}$ is the combined moment of inertia of the gimbal and the flywheel around the x-axis.) Because it it small, the influence of these other two components on the motion of the station can be neglected.

The torque generated by turning the gimbal is

$$\bar{L} = \dot{\bar{h}} + \Omega \times h$$
$$= [I_{G,x} \ddot{\delta} + I_s \Omega_s (q \cos \delta + r \sin \delta)] \cdot i$$
$$- [I_s \Omega_s \dot{\delta} \cos \delta + p I_s \Omega_s \cos \delta + r I_{G,x} \dot{\delta}] \cdot j$$
$$- [I_s \Omega_s \dot{\delta} \sin \delta + p I_s \Omega_s \sin \delta + q I_{G,x} \dot{\delta}] \cdot k$$

The j and k components of L, along with the centrifugal forces, constitute the load on the gimbal—and spin—bearings. Sufficient power must be provided to replace the energy dissipated by friction.

Because the station is rotating, $L_x \neq 0$. Power is therefore required to turn the gimbal:

$$P = L_x \cdot \dot{\delta}$$

This power builds up potential energy:

$$E = \int_0^{t(\delta)} L_x \dot{\delta} \, dt \approx \left[\frac{1}{2} I_{G,x} \dot{\delta}^2 \right]_{\dot{\delta}=0}^{\dot{\delta}=0} + I_s \cdot \Omega_s \int_0^{\delta} r \sin \delta \, d\delta$$

(q is neglected as small) or, considering r to be independent of δ:

$$E \approx I_s \cdot \Omega_s r (1 - \cos \delta)$$

and for $\delta = \frac{\pi}{2}$,

$$E \approx 82 \text{ watt sec}$$

This energy has only to be built up. As soon as the torque is removed, the gimbal swings back to the opposite deflection.

It may be advantageous to use moderate rates of rotation of the gyro. The stored kinetic energy would thus be small, allowing the control to be switched on and the gyro to be started as required. The stored kinetic energy for an angular impulse, $I_s \cdot \Omega_s$, of 130kg m^2 sec^{-1} is, given that $I_s = 2$kg m^2,

$$E = 4250 \text{ watt sec}$$

SECTION IV. EFFECT OF EXTERNAL TORQUES

Still to be mentioned are the effects of external torques. These have not been considered in our analyses mainly because external torques in space are small (gravity gradient, magnetic fields, radiation pressure, drag). They therefore change the angular impulse only very slowly:

$$L = \frac{dH}{dT}$$

The same can be said of the impact of meteoroids. Roll motion resulting from such impacts can be damped out as it occurs and the axis of rotation will be in line with the direction of the angular impulse.

Finally, it may occasionally be necessary to use jets to restore and maintain the desired rate of rotation and the direction in space of the axis of rotation.

SECTION V. CONCLUSIONS

Mass motion in a rotating space station of cylindrical shape causes the station to oscillate in the roll direction. The more nearly symmetrical the station is around its length axis, the larger the amplitude of the roll oscillation will be. But, as is shown in the example investigated, a difference even as small as 0.2% between the moments of inertia of the major and the intermediate axes suffices to keep the oscillation small. In addition, excessive roll can be reduced by control systems using a flywheel or corrective motion of the astronauts.

APPENDIX — *Orientation of the Principal Axes of the Space Station Relative to the Body-Fixed Axes*

The angular impulse is related to the angular velocity by

$$\bar{H}=\begin{vmatrix} I_x & -I_{xy} & -I_{xz} \\ -I_{xy} & I_y & -I_{yz} \\ -I_{xz} & -I_{yz} & I_z \end{vmatrix}\cdot\bar{\Omega} \qquad \text{(A)}$$

For H pointing in the direction of the principal axis,

$$\bar{H}=\lambda\bar{\Omega}$$

Writing this in components,

$$\begin{aligned} I_x p - I_{xy} q - I_{xz} r &= \lambda p \\ -I_{xy} p + I_y q - I_{yz} r &= \lambda q \\ -I_{xz} p - I_{yz} q + I_z r &= \lambda r \end{aligned} \qquad \text{(B)}$$

It follows that the determinant

$$\begin{vmatrix} (I_x-\lambda) & -I_{xy} & -I_{xz} \\ -I_{xy} & (I_y-\lambda) & -I_{yz} \\ -I_{xz} & -I_{yz} & (I_z-\lambda) \end{vmatrix}=0$$

This cubic equation in λ has three roots, λ_1, λ_2, λ_3, which correspond to I_ξ, I_η, I_ζ. The value for λ closest to I_x is I_ξ. Using $\lambda_1=I_\xi$, Equations (B) become

$$\begin{aligned} (I_x-I_\xi)\,p - I_{xy} q - I_{xz} r &= 0 \\ -I_{xy} p + (I_y-I_\xi)\,q - I_{yz} r &= 0 \\ -I_{xz} p - I_{yz} q + (I_z-I_\xi)\,r &= 0 \end{aligned}$$

The first equation can be interpreted as a scalar product $\bar{a}\cdot\bar{\Omega}=0$ indicating that $\bar{a}$ is perpendicular to $\bar{\Omega}$ with

$$\bar{a}=(I_x-I_\xi)\,i - I_{xy} j - I_{xz} k$$

The second equation yields a vector, $\bar{b}$, with

$$\bar{b}=-I_{xy} i + (I_y-I_\xi) j - I_{yz} k$$

The vector $\bar{a}\times\bar{b}$ has the direction of the principal axis ξ.

$$\bar{a}\times\bar{b}=\begin{vmatrix} i & j & k \\ (I_x-I_\xi) & -I_{xy} & -I_{xz} \\ -I_{xy} & (I_y-I_\xi) & -I_{yz} \end{vmatrix}$$

We can now express the orientation of the principal axes relative to the body-fixed axes by determining the three Euler angles α, β, γ. We use the same sequence of rotation as we used in converting from the reference axes to the body-fixed axes. The z-axis agrees with $\dot{\gamma}$, the ξ-axis with $\dot{\alpha}$. We can therefore use the matrix of Equation (1):

$$\begin{bmatrix}\Omega_\xi \\ \Omega_\eta \\ \Omega_\zeta\end{bmatrix}=\begin{bmatrix} \cos\beta\cos\gamma & \cos\beta\sin\gamma & -\sin\beta \\ \cos\gamma\sin\beta\sin\alpha-\sin\gamma\cos\alpha & \sin\alpha\sin\beta\sin\gamma+\cos\alpha\cos\gamma & \sin\alpha\cos\beta \\ \cos\alpha\sin\beta\cos\gamma+\sin\alpha\sin\gamma & \cos\alpha\sin\beta\sin\gamma-\sin\alpha\cos\gamma & \cos\alpha\cos\beta \end{bmatrix}\begin{bmatrix}p \\ q \\ r\end{bmatrix} \qquad \text{(C)}$$

Because $a\times b$ has the direction of the ξ-axis, its component $i\cdot\bar{a}\times\bar{b}$ is proportional to $\cos\gamma\cos\beta$ and its component $j\cdot\bar{a}\times\bar{b}$ is proportional to $\sin\gamma\cos\beta$. We determine γ for the ξ-axis (selecting the smallest γ) from

$$\frac{j\bar{a}\times\bar{b}}{i\bar{a}\times\bar{b}}=\frac{\sin\gamma\cos\beta}{\cos\gamma\cos\beta}=\tan\gamma=\frac{I_{yz}(I_x-I_\xi)+I_{xz}\cdot I_{xy}}{I_{yz}I_{xy}+I_{xz}(I_y-I_\xi)} \qquad \text{(D)}$$

We determine β from

$$\frac{k\bar{a}\times\bar{b}}{i\bar{a}\times\bar{b}}=\frac{-\sin\beta}{\cos\gamma\cos\beta}=-\frac{1}{\cos\gamma}\tan\beta \qquad \text{(E)}$$

$$=\frac{(I_x-I_\xi)(I_y-I_\xi)-I_{xy}^2}{I_{xy}I_{yz}+I_{xz}(I_y-I_\xi)}$$

To determine α, we rewrite Equations (2) using $\lambda_2=I\eta$,

$$\begin{aligned} (I_x-I_\eta)\,p - I_{xy} q - I_{xz} r &= 0 = \bar{c}\cdot\bar{\Omega} \\ -I_{xy} p + (I_y-I_\eta)\,q - I_{yz} r &= 0 = \bar{d}\cdot\bar{\Omega} \end{aligned}$$

and we use the relationship

$$\frac{j\bar{c}\times\bar{d}}{k\bar{c}\times\bar{d}}=\sin\gamma\tan\beta+\frac{\cos\gamma}{\cos\beta}\tan\alpha \qquad \text{(F)}$$

Because β, γ are small,

$$\frac{j\bar{c}\times\bar{d}}{k\bar{c}\times\bar{d}}\approx\tan\alpha$$

REFERENCES

1. Grantham, W. D., *Effects of Mass-Loading Variations and Applied Moments on Motion and Control of a Manned Rotating Space Vehicle,* NASA TN D-803 (1961).

2. Kurzhals, P. R. and C. R. Keckler, *Spin Dynamics of Manned Space Stations,* NASA TR R-155 (1963).

3. Adams, J. J., *Study of an Active Control System for a Spinning Body,* NASA TN D-905 (1961).

4. Whittaker, E. T., *A Treatise on the Analytical Dynamics of Particles and Rigid Bodies,* New York, Dover (1944).

5. Thomson, W. T., *Introduction to Space Dynamics,* New York, Wiley (1961).

6. Joos, Georg, *Theoretical Physics,* translated by I. M. Freeman, New York, Hafner (1958).

7. Goldstein, Herbert, *Classical Mechanics,* Cambridge, Mass., Addison-Wesley (1950).